Post-translational modification of ribosomally synthesized peptides by a radical SAM epimerase in Bacillus subtilis

Alhosna Benjdia, Alain Guillot, Pauline Ruffié, Jérôme Leprince, Olivier Berteau

Published in final edited form as:
Nat Chem. 2017 July ; 9(7): 698–707. doi:10.1038/nchem.2714.

Post-translational modification of ribosomally synthesized peptides by a radical SAM epimerase in *Bacillus subtilis*

Alhosna Benjdia[1], **Alain Guillot**[1], **Pauline Ruffié**[1], **Jérôme Leprince**[2], and **Olivier Berteau**[1,*]

[1]Micalis Institute, ChemSyBio, INRA, AgroParisTech, Université Paris-Saclay, 78350 Jouy-en-Josas, France

[2]Inserm U982, PRIMACEN, University of Rouen Normandy, F-76130 Mont-Saint-Aignan, France

Abstract

Ribosomally-synthesized peptides are built out of L-amino acids while D-amino acids are generally the hallmark of nonribosomal synthetic processes. Here we show that the model bacterium *Bacillus subtilis* is able to produce a novel type of ribosomally synthesized and post-translationally modified peptide containing D-amino acids that we propose to call epipeptides. We demonstrate that a two [4Fe-4S] clusters radical SAM enzyme converts L-amino acids into their D-counterparts by catalyzing C_α H-atom abstraction and using a critical cysteine residue as H-atom donor. Unexpectedly, these D-amino acid residues proved to be essential for the bioactivity of a peptide inducing the expression of LiaRS, a major component of the bacterial cell envelope stress response system. Present in *B. subtilis* and in several members of the human microbiome, these epipeptides and radical SAM epimerases broaden the landscape of peptidyl structures accessible to living organisms.

Bacterial cell envelop integrity is critical for bacteria survival and adaptation to the environment. Consequently, bacteria have developed several systems to sense membrane alterations. In *Bacillus subtilis*, a major cell envelope stress module is the Lia system composed of a two-component system (LiaRS) and an inhibitory protein (LiaF)1,2. This genetic system is highly conserved among Firmicutes and part of the complex regulatory network orchestrating the cell wall stress response1,2. Although its regulation has been described in great details, its precise physiological role in *B. subtilis* is not fully understood. LiaRS is specifically and strongly induced by antibiotics targeting the cell wall such as nisin, vancomycin or bacitracin3 and has been developed as a biosensor and high-throughput screen4. Upon antibiotic sensing, LiaRS transduces cell envelop stress signals activating

---

Correspondence and requests for materials should be addressed to O.B., INRA, Institut Micalis (UMR 1319), ChemSyBio, F-78350 Jouy-en-Josas, France. Tel. :+33(0)1 34 65 23 08, Fax : +33(0)1 34 65 24 62, Olivier Berteau Olivier.Berteau@jouy.inra.fr.

Author contributions

A.B. & O.B. conceived and designed the experiments; A.B., A.G., P.R., J.L and O.B performed the experiments; A.B., A.G, J.L and O.B. analyzed the data; A.B. & O.B. co-wrote the manuscript.

Competing financial interests

The authors declare no competing financial interests

Additional information

Reprints and permissions information is available online at www.nature.com/reprints.

Europe PMC Funders Author Manuscripts

gene expression presumably to maintain cell wall integrity. However, LiaRS does not appear to confer antibiotic resistance.

In an attempt to identify genes involved in LiaRS regulation, a mutagenesis study was undertaken in *B. subtilis* leading to the discovery of the *yydFGHIJ* operon5. This operon shows positive regulation on LiaRS and possesses all the characteristic features of a genetic system encoding a putative peptide (YydF) modified by a radical SAM enzyme (YydG) and a protease (YydH). The modified peptide is then predicted to be exported in the extracellular medium by an ABC-type transporter (YydIJ) even though none of these components has been isolated or investigated so far (Fig. 1a). Among these five genes, the function of the putative radical SAM enzyme (YydG) was unclear and predicted to be a peptide modifying enzyme5. However, it does not possess significant homology with any known radical SAM enzyme.

Radical SAM enzymes are emerging as a novel superfamily of enzymes catalyzing a broad range of radical-based reactions, many of them having no precedent in biology6–8. They are characterized by the presence of at least one [4Fe-4S] center which binds *S*-adenosyl-L-methionine (SAM) in a bidendate fashion *via* its carboxylate and amino moities9,10. Recent studies have highlighted the structural diversity of these enzymes which often contain additional [4Fe-4S] centers and/or cofactors such as PLP11 or cobalamin12. Upon reduction, the radical SAM $[4Fe\text{-}4S]^{1+}$ center transfers one electron to SAM resulting in its reductive fragmentation13 and usually, to the generation of the 5'-deoxyadenosyl radical (5'-dA$^{\bullet}$), although this species has never been characterized14. The 5'-dA$^{\bullet}$ then abstracts a substrate H-atom and, in most of the cases, leads to the formation of one equivalent of 5'-deoxyadenosine (5'-dA), although few enzymes, including lysine 2,3-aminomutase15 and spore photoproduct lyase16–18, have been reported to recycle SAM.

Radical SAM enzymes have been shown to be involved in a wide range of protein and peptide post-translational modifications including the formation of glycyl radicals19, oxidation20–23, methylthio transfer24,25 or thioether bond formation26,27. It is hence of no surprise if recent studies have highlighted their broad distribution in the biosynthetic pathways of the so-called RiPPs (ribosomally synthesized and post-translationally modified peptides)28, where they have been proposed to catalyze unprecedented reactions such as unusual methyl transfer29,30 or epimerization reactions29.

Results and Discussion

YydG is a two [4Fe-4S] cluster radical SAM enzyme catalyzing peptide post-translational modifications

To investigate the catalytic function of the putative radical SAM enzyme YydG and the biological role of the YydF peptide, we expressed the protein in *E. coli* and assayed its activity against YydF. The purified and anaerobically reconstituted protein had the distinctive spectroscopic properties of radical SAM enzymes with charge transfer absorption bands at 320 and 420 nm (Fig. 1b & c). Iron-sulfur determination indicated that, after anaerobic reconstitution, YydG contained 7.3± 0.1 Fe and 7.7± 0.5 sulfide per polypeptide chain, in agreement with the UV-visible spectrum of the protein (Fig. 1c & Supplementary

Fig. S1). These results supported that YydG contains two $[4Fe\text{-}4S]^{2+}$ centers. Anaerobic reduction of the reconstituted protein by sodium dithionite resulted in ~20% decreased intensity in the 350-700 nm region (Fig. 1c), similarly to what has been reported for the reduction of $[4Fe\text{-}4S]^{2+}$ to $[4Fe\text{-}4S]^{1+}$ cluster in other radical SAM enzymes31. As expected, exposure to atmospheric oxygen resulted in cluster re-oxidation as shown by the increase of the absorbance in the 350-700 nm region (Supplementary Fig. S1).

Genome mining revealed that *yydF* and *yydG* genes are also present in Gram-positive pathogens including *Enterococcus faecalis* and several *Staphylococcus* and *Streptococcus species* (Supplementary Fig. S2). Sequence alignment of selected YydF homologs indicated a highly conserved region from the residues 23 to the *C*-terminus end of the peptide (Fig. 1d and Supplementary Fig. S2). To probe the activity of YydG, we assayed the reconstituted enzyme with the full-length YydF peptide or a truncated form, encompassing the conserved amino acid residues from position 18 to 49 (peptide $YydF_{18\text{-}49}$). As shown, under anaerobic and reducing conditions, YydG converted ~30% of the YydF peptide (Supplementary Fig. S3) and >80% of the $YydF_{18\text{-}49}$ peptide (Fig. 1e) into several peptide products: $YydF_a$, $YydF_b$ and $YydF_c$ eluting at 41.7, 42.2 and 42.8 min, respectively. Concomitantly, SAM was converted into 5'-deoxyadenosine (5'-dA) during the reaction (Fig. 1f). As expected, if we omitted the enzyme or sodium dithionite, no peptide modification was observed, demonstrating the radical nature of the reaction (Supplementary Fig. S4). Interestingly, we also evidenced that YydG co-purified with large amounts of SAM as shown by HPLC analysis and SAM cleavage assay (Supplementary Fig. S5). Altogether, these results established that YydG is a two [4Fe-4S] centers radical SAM enzyme catalyzing the modification of the YydF and $YydF_{18\text{-}49}$ peptides.

Because $YydF_{18\text{-}49}$ was a more soluble substrate, we used this truncated peptide to characterize the modification catalyzed by YydG. Mass spectrometry inspection of the three peptides formed ($YydF_a$, $YydF_b$ and $YydF_c$) revealed no mass difference compared to the substrate ($YydF_{18\text{-}49}$ $[M+3H]^{3+}$ = 1258.3) (Fig. 1e). This result was consistent with previous report on radical SAM enzymes catalyzing isomerization15, substrate rearrangement17,18 or epimerization29. Tryptic peptide mapping of the substrate (*i.e.* $YydF_{18\text{-}49}$) gave three major products (**Peptide 1** $[M+H]^+$ = 931.7, **Peptide 2** $[M+2H]^{2+}$ = 592.6 and **Peptide** 3 $[M+H]^+$ = 768.6) eluting at 22, 27 and 19.2 min respectively (Fig. 2a). Comparison with the enzymatically modified peptide showed the formation of two additional peptides (named **Peptide 2*** and **Peptide 3***) having the same molecular weight as **Peptides 2** and **3** but eluting at 26.5 and 23.5 min, respectively (Fig. 2b). This result supported that YydG had introduced two modifications one located internally (in **Peptide 2**) and one in the *C*-terminus end of the peptide (in **Peptide 3**).

To identify the nature and position of the modifications catalyzed by YydG, we repeated the reaction in >90% deuterated buffer since radical SAM enzymes are known to abstract but also, in some cases, to exchange H-atoms during catalysis. In deuterated buffer, YydG produced a similar pattern of products (*i.e.* $YydF_a$, $YydF_b$ & $YydF_c$) with $YydF_c$ being the most abundant and $YydF_a$ the minor product (Fig. 2c). LC-MS analysis of the reaction showed that under these conditions, $YydF_a$ and $YydF_c$ had a molecular weight of $[M+3H]^{3+}$ = 1258.6 and $YydF_b$ a molecular weight of $[M+3H]^{3+}$ = 1259.0 corresponding to one and

two Dalton units more than the $YydF_{18-49}$ substrate ($[M+3H]^{3+}$ = 1258.3), respectively. This result unambiguously demonstrated that one deuterium atom was incorporated into $YydF_a$ and $YydF_c$ while two deuterium atoms were added into $YydF_b$. Tryptic peptide mapping allowed to localize deuterium incorporation exclusively in **Peptide 2*** and **Peptide 3*** whose molecular masses shifted by one Dalton unit (*i.e.* $[M+2H]^{2+}$ =593.0 and $[M+H]^{+}$ = 769.6, respectively) (Fig. 2d). LC-MS/MS fragmentation of these two peptides showed that one deuterium atom was incorporated in **Val_{36}** (as proved by the characteristic ions: y_1, y_2+1 and b_7, b_8+1) and one in **Ile_{44}** (as shown by identification of the ions: y_5 and y_6+1) (Fig. 2e) (see Supplementary Fig. S6-7 and Supplementary Tables S1-5 **for full assignment**). Altogether these results demonstrated that YydG catalyzes the replacement of two H-atoms located in **Val_{36}** and **Ile_{44}** by two solvent exchangeable H-atoms during catalysis.

YydG is a novel type of radical SAM epimerase

To determine the nature of the modification, we performed acid hydrolysis of the enzymatically modified peptides and analyzed the amino acid content by LC-MS/MS after derivatization with *N*-α-(2,4-dinitro-5-fluorophenyl)-L-valinamide (L-FDVA) (see Supplementary methods). The $YydF_{18-49}$ peptide contains one **Ile** and five **Leu** residues (Fig. 1d) which not only have the same molecular weight than **Ile** but also eluted at similar retention times. As shown on Figure 3a & b, optimized LC-MS/MS conditions allowed the separation and characterization of L-Ile, L-Leu and L-Val but also of their D-configured counterparts (D-allo-Ile, D-Leu and D-Val) as diastereoisomers. Analysis of the enzymatically modified peptides showed that, in addition to L-Ile and L-Leu, another product eluting at 27.7 min was formed corresponding to D-allo-Ile as shown by its retention time, its molecular weight and the formation of a major ion fragment at *m/z*= 366. 2 in H_2O buffer and *m/z*= 367.2 in D_2O buffer (Fig. 3a & c). The D-allo-Ile/L-Ile ratio ranged from 20% in deuterated buffer (Fig. 3a) to 70% under standard assay conditions (Supplementary Fig. S8). Among the other amino acids, we only identified valine as a mixture of L- and D-amino acids (Fig. 3b). To definitely assert the nature of the modification, we synthesized a peptide containing one D-Val and one D-allo-Ile at positions 36 and 44, respectively. Tryptic peptide mapping and amino acid analysis of this synthetic peptide perfectly reproduced the ones obtained with the enzymatically modified peptide (Supplementary Fig. S9-11). We hence demonstrated that YydG is a radical SAM peptide epimerase, the first one shown to be active *in vitro* on a peptide backbone.

YydG catalyzes C_α H-atom

Of major interest, when we analyzed by LC-MS/MS the D-amino acids produced in deuterated buffer, we monitored a mass increment of +1 Da only in D-allo-Ile and D-Val (Fig. 3c & d), supporting that the epimerization process resulted from the replacement of the C_α H-atom by a solvent exchangeable H-atom (Supplementary Fig. S10-11). Interestingly, the 5'-dA produced during the reaction in deuterated buffer contained no significant labeling, as shown by high-resolution LC-MS/MS (Supplementary Fig. S12). This result suggested that YydG abstracts a non-exchangeable H-atom and that a tight coupling occurred between SAM cleavage and peptide post-translational modification.

To further demonstrate that YydG catalyzes direct H-atom abstraction, we synthesized a peptide variant (**YydF$_{18-49}$-VD$_8$**) containing two perdeuterated valines in position 36 and 44. The replacement of L-Ile$_{44}$ by an L-Val residue mirrored what is found in several YydF variants (Supplementary Fig. S2) and simplified the labeling procedure. Incubation of YydG with this novel substrate ($[M+2H]^{2+}$= 1887.7) led to the formation of 3 products with a mass loss of one ($[M+2H]^{2+}$= 1887.2) or two ($[M+2H]^{2+}$= 1886.7) Dalton units (Fig. 3e & Supplementary Fig. S13). This result definitively established that residues 36 and 44 are the targets of the enzyme. More importantly, the 5'-dA produced in the presence of **YydF$_{18-49}$-VD$_8$** had a mass increment of +1 Da ($[M+H]^+$ = 253.1) (Fig. 3f) demonstrating that YydG catalyzes direct C_α H-atom abstraction. Of note, the magnitude of the labeling (>85%) confirmed the tight coupling between SAM cleavage and H-atom abstraction. This result was in sharp contrast with other radical SAM enzymes catalyzing peptide post-translational modifications which exhibit strong uncoupling between 5'-dA production and peptide modification22,27.

We further assayed the activity of YydG on synthetic peptides containing one or two epimerized amino acids. YydG was able to convert the mono-epimerized peptides but not the peptide containing two epimerized residues (Supplementary Fig. S14). This result proved that, contrary to the eukaryotic peptide epimerases32, the reaction catalyzed by YydG is irreversible. In addition, this showed that no other modification is catalyzed by YydG.

Based on these analyses, we were able to assign YydF$_a$ as a peptide containing a D-Val in position 36, YydF$_c$ as peptide containing a D-allo-Ile in position 44 and YydF$_b$ as peptide containing a D-Val and a D-allo-Ile in positions 36 and 44, respectively. Hence, YydG produces a mixture of peptides containing either one or two modified amino acids, with **Ile$_{44}$** being the favored target *in vitro* (Fig. 1e). Kinetic analysis of the reaction showed that YydG had an activity of 2.7 nmol.min^{-1}.mg^{-1} and of 1.7 nmol.min^{-1}.mg^{-1} for the production of 5'-dA and epimerized peptides, respectively, in line with its propensity to add 1 to 2 epimerizations during *in vitro* catalysis (Fig. 3g). A rate constant of 0.15 min^{-1} was determined, similar to what has been measured for other radical SAM enzymes catalyzing peptide modifications8. Altogether, these results supported that YydG uses one molecule of SAM to epimerize one amino acid residue through a radical-based mechanism.

YydG defines a novel type of radical SAM epimerases present within the human microbiome

Recently, it has been shown that during the biosynthesis of the so-called proteusins, putative radical SAM enzymes catalyze the *in vivo* epimerization of amino acid residues29,33. Beside the three cysteine residues from the radical SAM cluster, multiple sequence alignment failed to reveal any sequence homologies between YydG and the proteusin epimerases (Supplementary Fig. S15). Further analysis using the HHPred server showed that, in sharp contrast with known radical SAM enzymes catalyzing RiPP post-translational modifications, YydG is deprived of the recently identified RiPP precursor peptide recognition element (*i.e.* RRE or PqqD-like domain)34 (Supplementary Fig. S16). The RRE domain has been shown to be a critical component for interaction between a vast array of

enzymes and the leader peptides commonly encountered in RiPPs. Its absence in YydG is consistent with the unique ability of this enzyme to modify full length and truncated peptide substrates.

Another major difference between YydG and the proteusin epimerases is the presence in YydG of a putative SPASM-domain35,36. This domain is likely involved in the coordination of the second [4Fe-4S] center as predicted by structural modeling (Supplementary Fig. S17). Multiple sequence alignment failed to evidence such additional cluster in proteusin epimerases (Supplementary Fig. S15). Interestingly, a similar SPASM-domain has been identified in the carbohydrate epimerase NeoN catalyzing the last step in the biosynthesis of the aminoglycoside neomycin B37. To further probe the sequence and structural relationships between these enzymes, we performed a phylogenetic analysis38–40 including all known radical SAM epimerases and key representative members from the radical SAM superfamily of enzymes (Fig. 4a). Interestingly, YydG did not cluster with other epimerases (*i.e.* carbohydrate or proteusin epimerases) but with a sub-group of radical SAM enzymes recently shown to catalyze thioether bond formation (*i.e.* AlbA, SkfB & ThnB). This result appears meaningful considering that all these enzymes are predicted to abstract a C_α H-atom during catalysis26,27. Finally, Proteusins are large peptides (>150 amino acids) characterized by the presence of a nitrile hydratase-type leader peptide29,33 while YydF is a typical bacterial peptide.

Collectively, these data demonstrate that YydF is the member of a distinct family of RiPPs28 that we propose to call Epipeptides. Blast search retrieved 216 sequences homologous to YydG (E-value >60) in Gram-positive bacteria mainly related to the human microbiota (Supplementary Table S6). In support with this observation, search in the Human Microbiome Project database allowed retrieving peptides sharing high sequence identity with YydF. We further built an YydG sequence similarity network and a genome neighborhood network using the EFI-EST server41. The genome neighborhood network showed a strong association between YydG homologs and a putative peptidase and the two sub-units of an ABC transporter (Supplementary Fig. S18). This association was further confirmed by KEGG gene cluster prediction which revealed perfect co-occurrence between the 5 genes of the *yydFGHIJ* operon across *Bacillus*, *Staphylococcus*, *Corynebacterium* and *Streptococcus* species.

YydG contains a critical H-atom donor

The last question which remained to be solved was the origin of the exchangeable H-atom introduced during catalysis. Indeed, the carbon-centered radical produced by YydG, after C_α H-atom abstraction, was unlikely to interact with a buffer component. This highly reactive species is presumed to be kept sealed within the enzyme active-site. Close inspection of the YydG sequence pointed out that, in addition to the three cysteine residues from the radical SAM motif, only six cysteines were present in the protein sequence (Supplementary Fig. S19). One cysteine residue was adjacent to the radical SAM motif (*i.e.* **Cys_{22}**), two cysteine residues were side-by-side in the sequence (**Cys_{222}** and **Cys_{223}**) while the three other cysteine residues were reminiscent of motifs involved in the coordination of [4Fe-4S] centers35. Homology modeling showed that the 5 cysteine residues, located in the *C*-

terminal part of the protein, had a correct position for the coordination of a SPASM [4Fe-4S] center (Supplementary Fig. S17). To probe their function, we substituted Cys_{22}, Cys_{222}, Cys_{223} and the three cysteine residues of the radical SAM motif (Cys_{14}, Cys_{18} and Cys_{21}) by alanine residues. The four designed mutants (*i.e.***C22A**, **C222A, C223A and A3**) were successfully purified although the **C222A** mutant proved to be recalcitrant to purification and was produced partly as a truncated form (Fig. 4b). Spectroscopic analysis and iron assay showed that, in agreement with our structural model, the **A3** mutant contained after anaerobic reconstitution 4.6± 0.1 Fe and 5.7± 0.2 sulfide per polypeptide chain indicating the presence of one [4Fe-4S] center (Fig. 4c and Supplementary Fig. S17 & S20).

The UV-visible spectra of **C22A** and **C223A** mutants perfectly superimpose with the wild-type enzyme. The **C22A** mutant contained 8.6± 0.3 Fe and 7.9± 0.5 sulfide and the **C223A** mutant 8.2± 0.3 Fe and 7.1± 0.2 sulfide per polypeptide. In contrast, the **C222A** mutant did not contain detectable amounts of iron-sulfur center, even after anaerobic reconstitution (Fig. 4c & Supplementary Fig. S20). Furthermore, its absorption maximum was shifted toward 250 nm indicating that the protein was likely misfolded as reported for many radical SAM enzymes35,37, when cysteine residues involved in [4Fe-4S] coordination are mutated.

The activity of all the mutants was assayed under standard assay conditions with the $YydF_{18\text{-}49}$ substrate (Fig. 4d). As expected, the **A3** mutant was unable to cleave SAM and to convert the peptide substrate. Similarly, the activity of the **C222A** mutant was impaired consistent with the absence of [4Fe-4S] center in this enzyme. In contrast, the **C22A** mutation did not affect the activity of the enzyme as shown by the formation of the three epimerized peptides (*i.e.* $YydF_a$, $YydF_b$ and $YydF_c$) (Fig. 4d). The **C223A** mutant exhibited also enzyme activity. However, this enzyme variant showed a different pattern of products, with only the $YydF_c$ peptide being efficiently produced (Fig. 4d). If we substituted this residue by an isosteric serine residue (**C223S** mutant), the activity was further inhibited (Supplementary Fig. S21) suggesting a critical role for this residue.

These results were reminiscent of the spore photoproduct lyase (SP lyase), a radical SAM enzyme catalyzing DNA repair17. We and others have shown that SP lyase uses a cysteine residue to quench the radical substrate intermediate and terminate the reaction16–18,42. When mutated, SP lyase produced, along its expected product, several DNA adducts43. The structural study of SP lyase confirmed that a conserved cysteine residue was perfectly positioned to act as an H-atom donor18,42. Additional studies have shown that the activity of a mutated SP lyase could be rescued by precisely positioning a cysteine residue within the enzyme active site42.

We thus compared the activity of YydG (wild-type and **C223A** mutant) in the presence or the absence of DTT, a potential source of H-atoms. While the wild-type enzyme still produced the epimerized peptides, the C223A mutant produced other peptide derivatives in the absence of DTT (Fig. 4e). LC-MS analysis showed that these peptides derived from $YydF_{18\text{-}49}$ and contained a modified $\mathbf{Val_{36}}$ or $\mathbf{Ile_{44}}$ at their *N*-terminus or *C*-terminus ends with a mass shift of -30.005 Da and -1.032 Da (Fig. 4e & f, Supplementary Fig. S22-25).

We identified the modification as the loss of a carboxyl or amino group, resulting from the rupture of either the C_α-N or the C_α-CO bonds, and the addition of a double-bonded oxygen-atom on the C_α-atom (Fig. 4f). No other product, resulting from peptide cleavage, hydrolysis or rearrangement could match our MS analysis (Supplementary Table S7). The peptides were determined as being: **$I^{\Delta 1}$**LGSGH-NH_2 (peptide **$I_{44}^{\Delta 1}$-H_{49}**, $[M+Na]^+$= 603.2861), Ac-GLLDESQKLAKVNDLWYFVKSKENRW**$I^{\Delta 30}$** (peptide **G_{18}-$I_{44}^{\Delta 30}$**, $[M+2H]^{2+}$= 1646.3838) and Ac-GLLDESQKLAKVNDLWYF**$V^{\Delta 30}$** (peptide **G_{18}-$V_{36}^{\Delta 30}$**, $[M+2H]^{2+}$= 1125.7) (See Supplementary Fig. S22-25 & Supplementary Table S8-12 for full assignment and analysis).

These results were reminiscent of the oxygen-induced cleavage at the sites of the glycyl radical of the pyruvate formate lyase44 and the ribonucleotide reductase45. However, to date, the structure of these peptides containing an oxygen atom double-bonded to the C_α-atom is unique among radical SAM enzymes. Altogether, these results are in perfect agreement with our hypothesis that YydG generates a carbon-centered radical on the C_α-atom of **Val_{36}** and **Ile_{44}** and that Cys_{223} plays a critical role for the termination of the reaction. In light of previous work on SP lyase16–18,42,43, we interpret the role of Cys_{223} as the critical H-atom donor required for the termination of the reaction.

We propose an unprecedented mechanism on a peptide backbone leading to peptide epimerization (Fig. 5). After reductive cleavage of SAM, YydG generates a 5′-dA radical which abstracts the C_α H-atom of L-Val or L-Ile. This process is thermodynamically favourable considering the bond dissociation energies (BDE) of 354.6 and 351.3 $kJ.mol^{-1}$ for the H-C_α bonds of L-Val and L-Ile, respectively46. 5′-dA and a carbon-centered radical are then formed, leading to the loss of the C_α atom stereochemistry. This radical intermediate is then quenched by a thiol H-atom provided by a protein cysteine residue (*i.e.* Cys_{223}). Although the BDE of the thiol H-atom is slightly higher (368.8 $kJ.mol^{-1}$), such radical transfers have been extensively reported notably in the case of the ribonucleotide reductase47 and is supported here by the stable incorporation of a solvent derived H-atom into the peptide backbone. In addition, we showed that in the absence of this critical cysteine residue (Cys_{223}), polypeptide fragmentation occurs at the two radical sites leading to the formation of unusual peptide fragments. For the next catalytic cycle, the thiyl radical intermediate located on Cys_{223} has to be reduced. In the case of the carbohydrate epimerase NeoN37, it has been proposed that the reduction of the thiyl radical involves a remote cysteine and the formation of a disulfide anion radical, similarly to ribonucleotide reductase48. However, assuming the SPASM [4Fe-4S] center has full coordination, like in all characterized SPASM-domain radical SAM enzymes36, this would require bond breakage between a cysteine residue and the [4Fe-4S] center followed by further rearrangements. The proximity of a [4Fe-4S] center with a thiyl radical is reminiscent of ferredoxin:thioredoxin reductase49 and heterodisulfide reductases50,51 for which spectroscopic and structural52 studies have pointed that the function of a $[4Fe\text{-}4S]^{2+}$ center is to stabilize a thiyl radical leading to the formation of a pentacoordinated iron with unique properties50,53. A similar mechanism might be involved to reduce the thiyl radical generated on Cys_{223} during catalysis by YydG. In support of this hypothesis, we showed that the A3 mutant, containing only the SPASM [4Fe-4S] center, could not be reduced by

sodium dithionite (Supplementary Fig. S26), a typical feature of ferredoxin:thioredoxin reductase49 and heterodisulfide reductases53. Hence, we proposed that during catalysis, Cys_{223} might coordinate one Fe atom of the SPASM [4Fe-4S] center in order to regenerate the thiolate group for the next catalytic cycle.

Biological activity of the YydF epipeptide

Finally, since the *yydFGHIJ* operon (Fig. 1a) was shown to activate the *B. subtilis* Lia system, possibly by perturbing the bacterial cell wall5, we assayed the activity of the enzymatically modified $YydF_{18-49}$ peptide on *B. subtilis*. LB medium was inoculated with *B. subtilis* in the presence of peptide containing one, two or no epimerized residue. As shown, the unmodified $YydF_{18-49}$ peptide or the peptides containing either a **D-Val$_{36}$** or a **D-allo-Ile$_{44}$** ($YydF_a$ and $YydF_c$, respectively) did not affect the growth of *B. subtilis* (Fig. 6a). In sharp contrast, the peptide containing both a **D-Val$_{36}$** and a **D-allo-Ile$_{44}$** residue (**$YydF_b$**) strongly inhibited bacterial growth, supporting a key biological function for these 2 epimerized residues. We reproduced the experiment by adding $YydF_b$ during mid-exponential phase, when bacterial cells have reached a high density. As shown, addition of the two epimerized peptide led to a surprising fast decay of the bacterial population (Fig. 6b).

In order to demonstrate if *B. subtilis* actually produces epimerized peptides and to determine the relevant physiological form of the YydF peptide, we tried to isolate the naturally secreted peptide. Large scale transcriptomic analysis designed to cover various adaptative features of *B. subtilis* revealed that *yydF* is strongly expressed under nutrient depletion conditions54 (Supplementary Fig. S27). We grew *B. subtilis* in synthetic medium under conditions favoring optimal induction of the *yydF*, *yydG*, *yydH*, *yydI* and *yydJ* genes54 (*see Supplementary information*). The supernatant was purified by solid phase extraction and peptides were searched by mass spectrometry analysis using the X!tandem suite55 and manual inspection. Only one relevant peptide ($[M+3H]^{3+}$: 703.1; Fig. 6c) was identified. The sequence of this 17mer peptide was determined to encompass residues 33 to 49 including the highly conserved domain found in YydF and the two amino acid residues, target of YydG (Fig. 6c and Supplementary Fig. S28). In order to determine if the purified peptide was actually epimerized, we synthesized two peptides containing either only L-amino acid residues (**$YydF_{33-49}$**) or a D-Val and a D-allo-Ile (**$YydF_{33-49DD}$**) in position 36 and 44 (respective positions to YydF). Interestingly, the peptide isolated from *B. subtilis* exhibited the same fragmentation pattern than the synthetic peptide **$YydF_{33-49DD}$** containing two D-amino acid residues (Supplementary Fig. S28). In addition, the retention time of the peptide isolated from *B. subtilis* (20.5 min) perfectly matched with the retention time of **$YydF_{33-49DD}$** but not with the one of **$YydF_{33-49}$** (18.7 min) (Fig. 6d). Finally, a tryptic peptide obtained after digestion of the peptide produced by *B. subtilis* eluted at the same time than **Peptide 3***, containing a D-allo-Ile (Supplementary Fig. S29). Altogether, these results demonstrate that *B. subtilis* produces peptides containing D-amino acids.

Finally, since we identified the mature form of YydF, we aimed at comparing its activity with the previously synthesized epimerized peptide (**$YydF_b$**). Surprisingly, **$YydF_{33-49DD}$** proved to be a stronger inhibitor leading to the total inhibition of *B. subtilis* growth (Fig. 6e).

Consistent with our previous experiments, a peptide with identical sequence but devoid of D-amino acid residues did not exhibited activity toward *B. subtilis* (Fig. 6e). In order to determine the minimum inhibitory concentrations (MIC) of **YydF$_{b}$** and **YydF$_{33\text{-}49DD}$**, we performed serial dilution assay. **YydF$_{33\text{-}49DD}$** proved to be at least 100 times more potent than **YydF$_{b}$** with a MIC < 2μg.mL^{-1} (Fig. 6f & g). This value is 120 times smaller than the MIC determined for bacitracin56, a well-known antibiotic peptide inducing LiaRS57 and inhibiting *B. subtilis* growth. To the best of our knowledge, it is the first time that a naturally short epimerized peptide, proved to be the active form of a bacterial peptide with regulatory and/or antimicrobial activity. Interestingly, the activity of **YydF$_{33\text{-}49DD}$** is in the range of the most potent inhibitory peptides58.

Although the physiological role of YydF has yet to be deciphered, its expression is perfectly correlated with *sdpC*, a gene encoding a *B. subtilis* killing factor59. Among the 4175 genes of *B. subtilis* no other gene exhibits a better correlation (Supplementary Fig. S27). Interestingly, the expression of both genes has been reported to be under the negative regulation of AbrB, a regulator of the central metabolism59. It is tempting to speculate that YydF is a novel regulator of *B. subtilis* complex metabolic plasticity. Our data support that the YydF peptide is first epimerized by the radical SAM enzyme YydG, processed by the YydH membrane protease and then exported by the YydIJ ABC-transporter. In support of this conclusion, assays performed between the YydG epimerase and the short YydF$_{33\text{-}49}$ peptide, revealed only low level of activity suggesting that it is not a relevant enzyme substrate.

Conclusion

This study demonstrates that peptides containing D-amino acids, are much more widespread in living organisms than previously anticipated. Indeed, recent reports suggested that such type of modification was restricted to bacteria with exceptional metabolic capacities such *Entotheonella* and related organisms producing proteusins60. We show here that epimerized peptides are also produced by the model bacterium *B. subtilis* and likely by several pathogenic species and members of the human microbiome including *Enterococcus faecalis*, *Streptococcus agalactiae* and *Staphylococcus epidermidis*.

Among known bio-active peptides and bacteriocins61, YydF represents the first member of a novel class of RiPPs, that we propose to call epipeptides. As we demonstrated here, the activity of epipeptides is dependent only of discrete epimerizations and requires no other post-translational modification. Peptides containing D-amino acids have thus to be considered when trying to identify the active forms of bacterial peptides with unknown functions notably within the human microbiome. Finally, radical SAM enzymes appear to be widespread catalysts employed by bacteria to increase peptide diversity through the control of the chirality of life.

Methods

Protein cloning & purifications, enzymatic assays, analytical techniques & peptide synthesis are described in Supplementary Information.

Supplementary Material

Refer to Web version on PubMed Central for supplementary material.

Acknowledgements

This work was supported by grants from European Research Council (ERC) (Consolidator Grant 617053 to OB). High resolution MS analyses were performed on INRA PAPPSO proteomics platform.

References

1. Jordan S, Junker A, Helmann JD, Mascher T. Regulation of LiaRS-dependent gene expression in bacillus subtilis: identification of inhibitor proteins, regulator binding sites, and target genes of a conserved cell envelope stress-sensing two-component system. J Bacteriol. 2006; 188:5153–66. [PubMed: 16816187]
2. Jordan S, Hutchings MI, Mascher T. Cell envelope stress response in Gram-positive bacteria. FEMS Microbiol Rev. 2008; 32:107–46. [PubMed: 18173394]
3. Mascher T, Margulis NG, Wang T, Ye RW, Helmann JD. Cell wall stress responses in Bacillus subtilis: the regulatory network of the bacitracin stimulon. Mol Microbiol. 2003; 50:1591–604. [PubMed: 14651641]
4. Mascher T, Zimmer SL, Smith TA, Helmann JD. Antibiotic-inducible promoter regulated by the cell envelope stress-sensing two-component system LiaRS of Bacillus subtilis. Antimicrob Agents Chemother. 2004; 48:2888–96. [PubMed: 15273097]
5. Butcher BG, Lin YP, Helmann JD. The yydFGHIJ operon of Bacillus subtilis encodes a peptide that induces the LiaRS two-component system. J Bacteriol. 2007; 189:8616–25. [PubMed: 17921301]
6. Benjdia A, Berteau O. Sulfatases and radical SAM enzymes: emerging themes in glycosaminoglycan metabolism and the human microbiota. Biochem Soc Trans. 2016; 44:109–15. [PubMed: 26862195]
7. Vey JL, Drennan CL. Structural insights into radical generation by the radical SAM superfamily. Chem Rev. 2011; 111:2487–506. [PubMed: 21370834]
8. Broderick JB, Duffus BR, Duschene KS, Shepard EM. Radical S-adenosylmethionine enzymes. Chem Rev. 2014; 114:4229–317. [PubMed: 24476342]
9. Walsby CJ, et al. Electron-nuclear double resonance spectroscopic evidence that S-adenosylmethionine binds in contact with the catalytically active [4Fe-4S](+) cluster of pyruvate formate-lyase activating enzyme. J Am Chem Soc. 2002; 124:3143–51. [PubMed: 11902903]
10. Nicolet Y, Amara P, Mouesca JM, Fontecilla-Camps JC. Unexpected electron transfer mechanism upon AdoMet cleavage in radical SAM proteins. Proc Natl Acad Sci U S A. 2009; 106:14867–71. [PubMed: 19706452]
11. Frey PA, Hegeman AD, Ruzicka FJ. The Radical SAM Superfamily. Crit Rev Biochem Mol Biol. 2008; 43:63–88. [PubMed: 18307109]
12. Pierre S, et al. Thiostrepton tryptophan methyltransferase expands the chemistry of radical SAM enzymes. Nat Chem Biol. 2012; 8:957–9. [PubMed: 23064318]
13. Wang SC, Frey PA. Binding energy in the one-electron reductive cleavage of S-adenosylmethionine in lysine 2,3-aminomutase, a radical SAM enzyme. Biochemistry. 2007; 46:12889–95. [PubMed: 17944492]
14. Horitani M, et al. Why Nature Uses Radical SAM Enzymes so Widely: Electron Nuclear Double Resonance Studies of Lysine 2,3-Aminomutase Show the 5'-dAdo* “Free Radical” Is Never Free. J Am Chem Soc. 2015; 137:7111–21. [PubMed: 25923449]
15. Wang SC, Frey PA. S-adenosylmethionine as an oxidant: the radical SAM superfamily. Trends Biochem Sci. 2007; 32:101–10. [PubMed: 17291766]
16. Chandor A, et al. Dinucleotide spore photoproduct, a minimal substrate of the DNA repair spore photoproduct lyase enzyme from Bacillus subtilis. J Biol Chem. 2006; 281:26922–31. [PubMed: 16829676]

17. Benjdia A. DNA photolyases and SP lyase: structure and mechanism of light-dependent and independent DNA lyases. Curr Opin Struct Biol. 2012; 22:711–20. [PubMed: 23164663]
18. Benjdia A, Heil K, Barends TR, Carell T, Schlichting I. Structural insights into recognition and repair of UV-DNA damage by Spore Photoproduct Lyase, a radical SAM enzyme. Nucleic Acids Res. 2012; 40:9308–18. [PubMed: 22761404]
19. Sun X, et al. The free radical of the anaerobic ribonucleotide reductase from Escherichia coli is at glycine 681. J Biol Chem. 1996; 271:6827–31. [PubMed: 8636106]
20. Benjdia A, Deho G, Rabot S, Berteau O. First evidences for a third sulfatase maturation system in prokaryotes from E. coli aslB and ydeM deletion mutants. FEBS Lett. 2007; 581:1009–14. [PubMed: 17303125]
21. Benjdia A, et al. Anaerobic sulfatase-maturating enzymes: radical SAM enzymes able to catalyze in vitro sulfatase post-translational modification. J Am Chem Soc. 2007; 129:3462–3. [PubMed: 17335281]
22. Benjdia A, Leprince J, Sandstrom C, Vaudry H, Berteau O. Mechanistic investigations of anaerobic sulfatase-maturating enzyme: direct Cbeta H-atom abstraction catalyzed by a radical AdoMet enzyme. J Am Chem Soc. 2009; 131:8348–9. [PubMed: 19489556]
23. Benjdia A, et al. Anaerobic sulfatase-maturating enzymes - first dual substrate radical S-adenosylmethionine enzymes. J Biol Chem. 2008; 283:17815–17826. [PubMed: 18408004]
24. Arragain S, et al. Post-translational modification of ribosomal proteins: structural and functional characterization of RimO from Thermotoga maritima, a radical-SAM methylthiotransferase. J Biol Chem. 2009
25. Lee KH, et al. Characterization of RimO, a new member of the methylthiotransferase subclass of the radical SAM superfamily. Biochemistry. 2009; 48:10162–74. [PubMed: 19736993]
26. Flühe L, K TA, Gattner MJ, Schäfer A, Burghaus O, Linne U, Marahiel MA. The radical SAM enzyme AlbA catalyzes thioether bond formation in subtilosin A. Nat Chem Biol. 2012; 8:350–7. [PubMed: 22366720]
27. Benjdia A, et al. Thioether bond formation by SPASM domain radical SAM enzymes: Calpha H-atom abstraction in subtilosin A biosynthesis. Chem Commun (Camb). 2016; 52:6249–52. [PubMed: 27087315]
28. Arnison PG, et al. Ribosomally synthesized and post-translationally modified peptide natural products: overview and recommendations for a universal nomenclature. Nat Prod Rep. 2013; 30:108–60. [PubMed: 23165928]
29. Freeman MF, et al. Metagenome mining reveals polytheonamides as posttranslationally modified ribosomal peptides. Science. 2012; 338:387–90. [PubMed: 22983711]
30. Huo L, Rachid S, Stadler M, Wenzel SC, Muller R. Synthetic biotechnology to study and engineer ribosomal bottromycin biosynthesis. Chem Biol. 2012; 19:1278–87. [PubMed: 23021914]
31. Duin EC, et al. [2Fe-2S] to [4Fe-4S] cluster conversion in Escherichia coli biotin synthase. Biochemistry. 1997; 36:11811–20. [PubMed: 9305972]
32. Bansal PS, et al. Substrate specificity of platypus venom L-to-D-peptide isomerase. J Biol Chem. 2008; 283:8969–75. [PubMed: 18158286]
33. Morinaka BI, et al. Radical S-adenosyl methionine epimerases: regioselective introduction of diverse D-amino acid patterns into peptide natural products. Angew Chem Int Ed Engl. 2014; 53:8503–7. [PubMed: 24943072]
34. Burkhart BJ, Hudson GA, Dunbar KL, Mitchell DA. A prevalent peptide-binding domain guides ribosomal natural product biosynthesis. Nat Chem Biol. 2015; 11:564–70. [PubMed: 26167873]
35. Benjdia A, et al. Anaerobic sulfatase-maturating enzyme--a mechanistic link with glycyl radical-activating enzymes? FEBS J. 2010; 277:1906–20. [PubMed: 20218986]
36. Grell TA, Goldman PJ, Drennan CL. SPASM and twitch domains in S-adenosylmethionine (SAM) radical enzymes. J Biol Chem. 2015; 290:3964–71. [PubMed: 25477505]
37. Kudo F, Hoshi S, Kawashima T, Kamachi T, Eguchi T. Characterization of a radical S-adenosyl-L-methionine epimerase, NeoN, in the last step of neomycin B biosynthesis. J Am Chem Soc. 2014; 136:13909–15. [PubMed: 25230155]
38. Kumar S, Stecher G, Tamura K. MEGA7: Molecular Evolutionary Genetics Analysis version 7.0 for bigger datasets. Mol Biol Evol. 2016

Europe PMC Funders Author Manuscripts

39. Jones DT, Taylor WR, Thornton JM. The rapid generation of mutation data matrices from protein sequences. Comput Appl Biosci. 1992; 8:275–82. [PubMed: 1633570]
40. Zharkikh A, Li WH. Estimation of confidence in phylogeny: the complete-and-partial bootstrap technique. Mol Phylogenet Evol. 1995; 4:44–63. [PubMed: 7620635]
41. Gerlt JA, et al. Enzyme Function Initiative-Enzyme Similarity Tool (EFI-EST): A web tool for generating protein sequence similarity networks. Biochim Biophys Acta. 2015; 1854:1019–37. [PubMed: 25900361]
42. Benjdia A, Heil K, Winkler A, Carell T, Schlichting I. Rescuing DNA repair activity by rewiring the H-atom transfer pathway in the radical SAM enzyme, spore photoproduct lyase. Chem Commun (Camb). 2014; 50:14201–4. [PubMed: 25285338]
43. Chandor-Proust A, et al. DNA repair and free radicals, new insights into the mechanism of spore photoproduct lyase revealed by single amino acid substitution. J Biol Chem. 2008; 283:36361–8. [PubMed: 18957420]
44. Wagner AF, Frey M, Neugebauer FA, Schafer W, Knappe J. The free radical in pyruvate formate-lyase is located on glycine-734. Proc Natl Acad Sci U S A. 1992; 89:996–1000. [PubMed: 1310545]
45. Reichard P, Ehrenberg A. Ribonucleotide reductase--a radical enzyme. Science. 1983; 221:514–9. [PubMed: 6306767]
46. Moore BN, Julian RR. Dissociation energies of X-H bonds in amino acids. Phys Chem Chem Phys. 2012; 14:3148–54. [PubMed: 22286066]
47. Stubbe J, Nocera DG, Yee CS, Chang MC. Radical initiation in the class I ribonucleotide reductase: long-range proton-coupled electron transfer? Chem Rev. 2003; 103:2167–201. [PubMed: 12797828]
48. Stubbe J, van der Donk WA. Ribonucleotide reductases: radical enzymes with suicidal tendencies. Chem Biol. 1995; 2:793–801. [PubMed: 8807812]
49. Staples CR, et al. The function and properties of the iron-sulfur center in spinach ferredoxin: thioredoxin reductase: a new biological role for iron-sulfur clusters. Biochemistry. 1996; 35:11425–34. [PubMed: 8784198]
50. Bennati M, Weiden N, Dinse KP, Hedderich R. (57)Fe ENDOR spectroscopy on the iron-sulfur cluster involved in substrate reduction of heterodisulfide reductase. J Am Chem Soc. 2004; 126:8378–9. [PubMed: 15237985]
51. Duin EC, Madadi-Kahkesh S, Hedderich R, Clay MD, Johnson MK. Heterodisulfide reductase from Methanothermobacter marburgensis contains an active-site [4Fe-4S] cluster that is directly involved in mediating heterodisulfide reduction. FEBS Lett. 2002; 512:263–8. [PubMed: 11852093]
52. Dai S, Schwendtmayer C, Schurmann P, Ramaswamy S, Eklund H. Redox signaling in chloroplasts: cleavage of disulfides by an iron-sulfur cluster. Science. 2000; 287:655–8. [PubMed: 10649999]
53. Walters EM, et al. Spectroscopic characterization of site-specific [Fe(4)S(4)] cluster chemistry in ferredoxin:thioredoxin reductase: implications for the catalytic mechanism. J Am Chem Soc. 2005; 127:9612–24. [PubMed: 15984889]
54. Nicolas P, et al. Condition-dependent transcriptome reveals high-level regulatory architecture in Bacillus subtilis. Science. 2012; 335:1103–6. [PubMed: 22383849]
55. Craig R, Cortens JC, Fenyo D, Beavis RC. Using annotated peptide mass spectrum libraries for protein identification. J Proteome Res. 2006; 5:1843–9. [PubMed: 16889405]
56. Radeck J, et al. Anatomy of the bacitracin resistance network in Bacillus subtilis. Mol Microbiol. 2016; 100:607–20. [PubMed: 26815905]
57. Wolf D, Dominguez-Cuevas P, Daniel RA, Mascher T. Cell envelope stress response in cell wall-deficient L-forms of Bacillus subtilis. Antimicrob Agents Chemother. 2012; 56:5907–15. [PubMed: 22964256]
58. Ling LL, et al. A new antibiotic kills pathogens without detectable resistance. Nature. 2015; 517:455–9. [PubMed: 25561178]

59. Ellermeier CD, Hobbs EC, Gonzalez-Pastor JE, Losick R. A three-protein signaling pathway governing immunity to a bacterial cannibalism toxin. Cell. 2006; 124:549–59. [PubMed: 16469701]

60. Wilson MC, et al. An environmental bacterial taxon with a large and distinct metabolic repertoire. Nature. 2014; 506:58–62. [PubMed: 24476823]

61. Cotter PD, Ross RP, Hill C. Bacteriocins - a viable alternative to antibiotics? Nat Rev Microbiol. 2013; 11:95–105. [PubMed: 23268227]

Europe PMC Funders Author Manuscripts

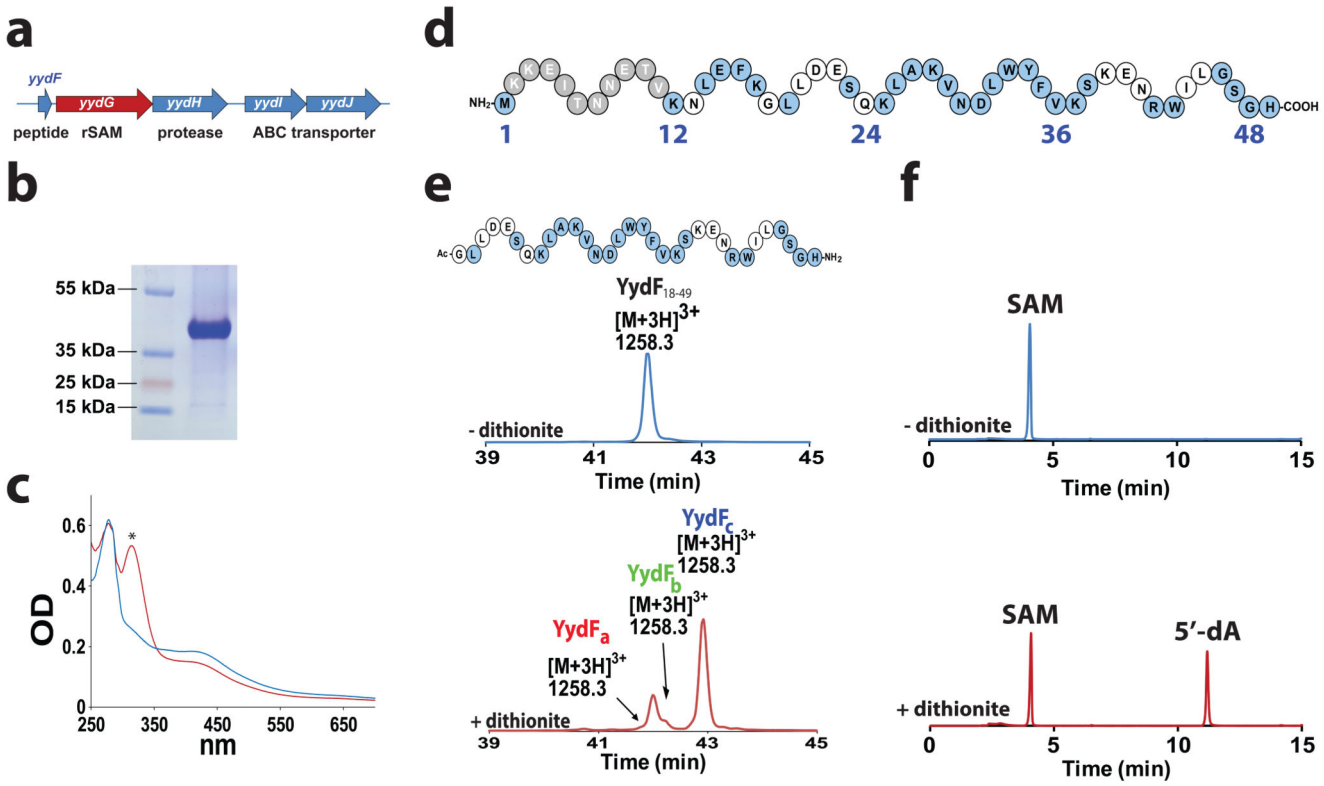

Figure 1. YydG is a radical SAM enzyme catalyzing the modification of the YydF peptide.

(a) Structure of the yydFGHIJ operon. *yydF*: putative peptide, *yydG*: radical SAM enzyme, *yydH*: protease, *yydIJ* ABC-type transporter. **(b) Gel electrophoresis analysis of purified YydG expressed in *E. coli*. (c) UV-visible spectrum of anaerobically reconstituted YydG (blue line) and reduced with sodium dithionite (red line).** The symbol * indicates absorbance due to reduced sodium dithionite. **(d) Sequence of the YydF peptide from *B. subtilis***. In grey, region with a low conservation; in blue, strictly conserved amino acid residues (*see* Supplementary Fig. S2). **(e) HPLC analysis of $YydF_{18\text{-}49}$ incubated with YydG after 90 min under anaerobic conditions in the absence (upper trace) or the presence (lower trace) of sodium dithionite as one-electron donor.** In the absence of sodium dithionite (upper trace), only the $YydF_{18\text{-}49}$ peptide substrate was monitored. The *m/z* of each peptide is indicated above the corresponding peaks. *See* Supplementary Information *for experimental conditions*. **(f) HPLC analysis of SAM incubated with YydG and $YydF_{18\text{-}49}$ after 90 min under anaerobic conditions in the absence (upper trace) or in the presence (lower trace) of sodium dithionite.** *See* Supplementary Information *for experimental conditions*.

Europe PMC Funders Author Manuscripts

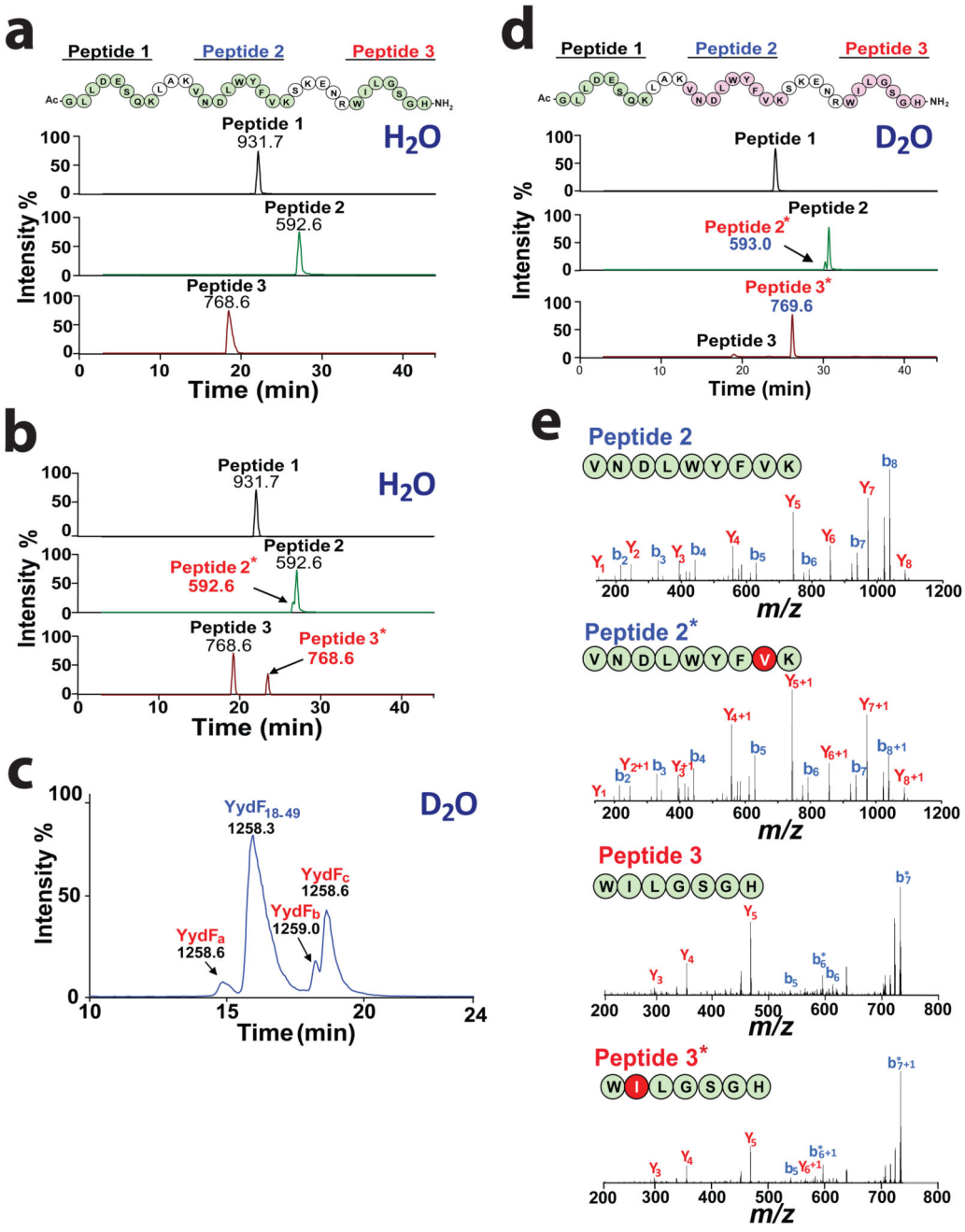

Figure 2. YydG catalyzes H-atom transfer to the peptide backbone.

Tryptic peptide mapping and LC-MS analysis of (a) YydF$_{18-49}$ or (b) YydF$_{18-49}$ after incubation with YydG. Numbers indicate the m/z value for each peptide. Sequences in green indicate the relevant peptide identified by LC-MS (*i.e.* **Peptide 1**: Ac-GLLDESQK, $[M+H]^+$ = 931.7 ; **Peptide 2**: VNDLWYFVK $[M+2H]^{2+}$ =592.6 and **Peptide 3:** WILGSGH-NH_2, $[M+H]^+$ =768.6). Sequences in pink represent the peptides modified by YydG. **(c) LC-MS analysis of the peptide YydF$_{18-49}$ after incubation with YydG in deuterated buffer**. **(d) Tryptic peptide mapping and LC-MS analysis of YydF$_{18-49}$ after incubation with**

YydG in deuterated buffer. (e) LC-MS/MS analysis of Peptide 2 (upper left panel), **Peptide 2*** (lower left panel), **Peptide 3** (upper right panel) and **Peptide 3*** (lower right panel) **obtained after tryptic hydrolysis of YydF$_{18-49}$ incubated with YydG in deuterated buffer** (see full assignment in Supplementary Table S2-5).

Europe PMC Funders Author Manuscripts

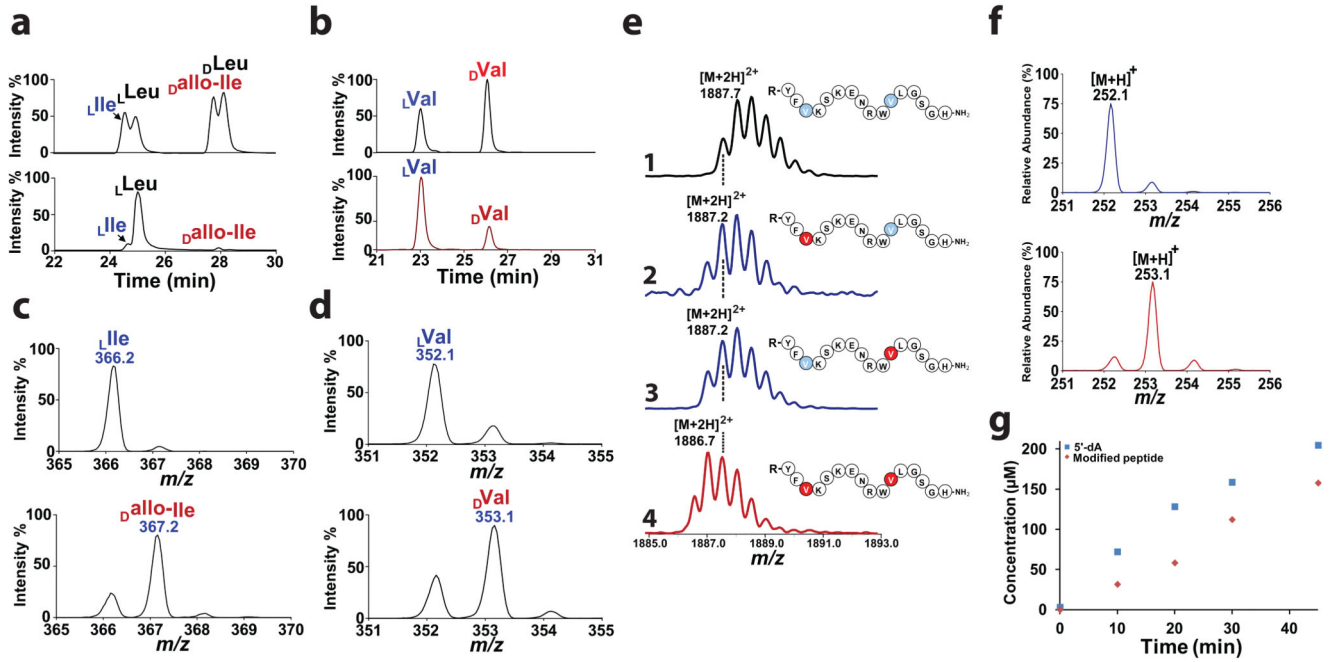

Figure 3. YydG catalyzes amino acid epimerization.

LC-MS/MS analysis of (a) L-/D-Leu and L-Ile/D-allo-Ile or (b) L-/D-Val. Upper traces were obtained with standard amino acids while lower traces correspond to amino acids obtained after incubation of $YydF_{18\text{-}49}$ with the radical SAM enzyme YydG in deuterated buffer. Amino acids were analyzed after hydrolysis and derivatization by *N*-α-(2,4-dinitro-5-fluorophenyl)-L-valinamide (L-FDVA). **MS spectra of (c) L-Ile-FDVA, (d) L-Val-FDVA (upper traces) and their D-epimers (lower traces) obtained after incubation of $YydF_{18\text{-}49}$ with YydG in deuterated buffer.** Mass spectra correspond to the dominant ions fragments: *m/z*= 366 and 352 for Ile- and Val-FDVA derivatives, respectively. The amino acids were derivatized by L-FDVA and detected by LC-MS after ion current extraction in MS/MS experiments using the transition 412>366 and 398>352 for Ile/Leu and Val-FDVA derivatives, respectively. (**e**) **LC-MS/MS analysis of the deuterated peptide $YydF_{18\text{-}49}$-VD_8 incubated with YydG.** After incubation with YydG, $YydF_{18\text{-}49}$-VD_8 ($[M+2H]^{2+}$ = 1887.7) (trace 1) was converted in peptides containing one D-valine ($[M+2H]^{2+}$ = 1887.2) (traces 2&3) or two D-Val $[M+2H]^{2+}$ = 1886.7 (trace 4). In the sequences, the octadeuterated L-valine residues are labeled in light blue and the heptadeuterated D-valine in red. Masses indicate mono-isotopic ions. **(f) LC-MS/MS analysis of 5'-dA produced by YydG incubated with $YydF_{18\text{-}49}$ (upper trace) or $YydF_{18\text{-}49}$-VD_8 (lower trace). (g) Time-course production of 5'-dA (blue symbol) and epimerized peptide (red symbol).** *See* supplementary Information *for experimental conditions*.

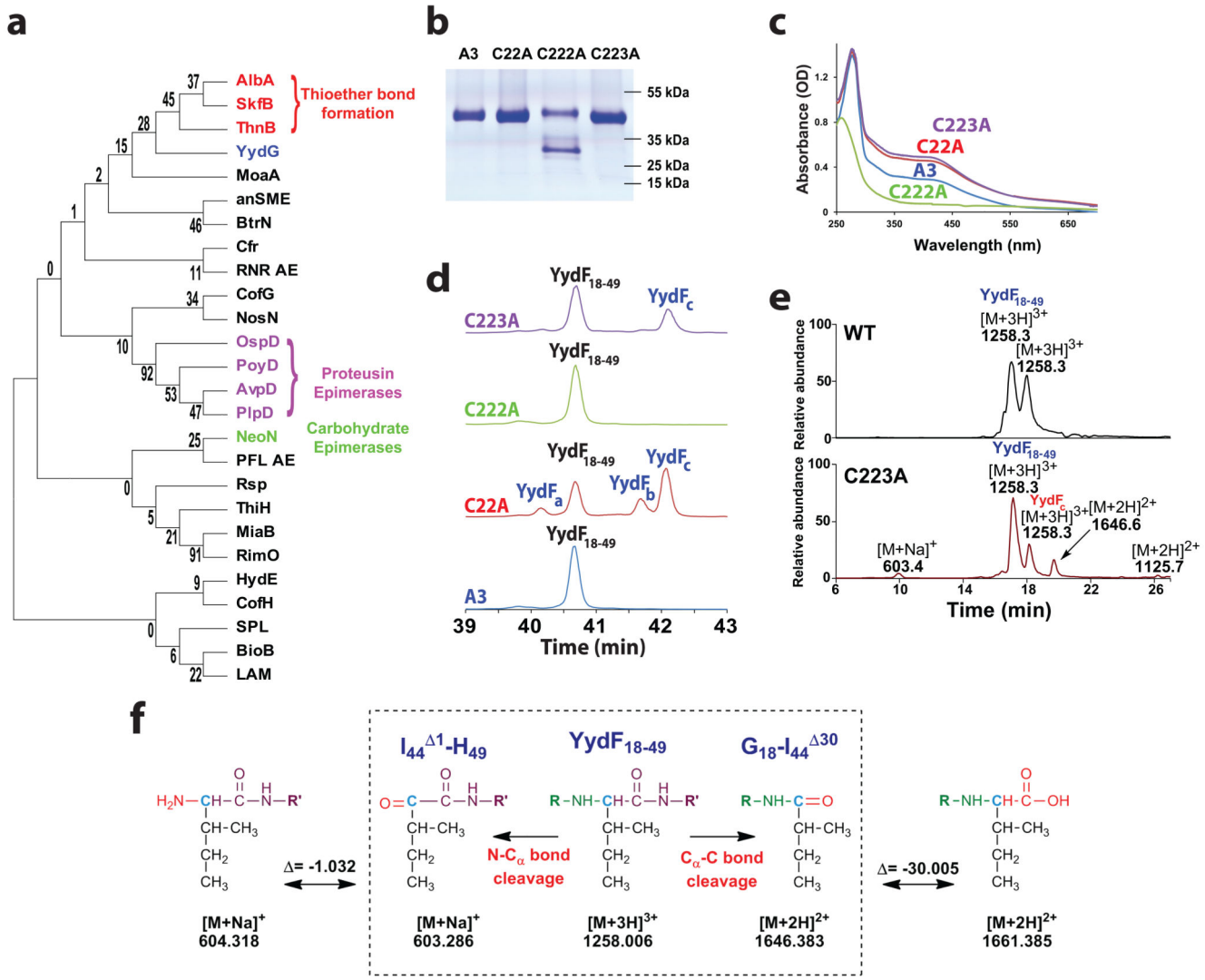

Figure 4. Activity of YydG mutants.

(**a**) **Molecular phylogenetic analysis of radical SAM epimerases and representative members of the radical SAM enzyme superfamily:** The evolutionary history was inferred by using the Maximum Likelihood method based on the JTT matrix-based mode39. The percentage of replicate trees in which the associated taxa clustered together in the bootstrap test40 (1000 replicates) are shown next to the branches. Initial tree(s) for the heuristic search were obtained by applying Neighbor-Join and BioNJ algorithms to a matrix of pairwise distances estimated using a JTT model, and then selecting the topology with superior log likelihood value (*see* Supplementary Information *for full methodology*. **(b) Gel electrophoresis analysis of the purified YydG mutants**. Mutants AxxxAxxA (**A3**), **C22A**, **C222A** and **C223A**. **(c) UV-visible spectra of A3 (blue trace), C22A (red trace), C222A (green trace) and C223A (purple trace) mutants after anaerobic reconstitution. (d) HPLC analysis of the reaction after incubation of YydF$_{18-49}$ and each mutant protein.** (**e**) **LC-MS analysis of the reaction catalyzed by the wild-type enzyme or the C223A**

Europe PMC Funders Author Manuscripts

mutant in the absence of DTT. YydG produced peptides at $[M+3H]^{3+}$= 1258.3 while the C223A mutants produced additional peptides at $[M+Na]^{+}$ = 603.2861, $[M+2H]^{2+}$= 1646.3838 and $[M+2H]^{2+}$= 1125.7 identified as $\mathbf{I_{44}^{\Delta 1}\text{-}H_{49}}$, $\mathbf{G_{18}\text{-}I_{44}^{\Delta 30}}$ and $\mathbf{G_{18}\text{-}V_{36}^{\Delta 30}}$, respectively (*see* Supplementary Fig. S22-25 and Supplementary Table S7-12 *for full analysis and assignment)*. (**f**) **Radical fragmentation mechanism of the $\mathbf{YydF_{18\text{-}49}}$ peptide leading to the production of the $\mathbf{I_{44}^{\Delta 1}\text{-}H_{49}}$ and the $\mathbf{G_{18}\text{-}I_{44}^{\Delta 30}}$.** The theoretical masses for the hydrolytic products (I_{44}-H_{49} & G_{18}-I_{44}) and the experimental masses measured ($I_{44}^{\Delta 1}$-H_{49} & G_{18}-$I_{44}^{\Delta 30}$) are indicated (*See* Supplementary Table S7 *for comparison with theoretical products*).

Europe PMC Funders Author Manuscripts

Europe PMC Funders Author Manuscripts

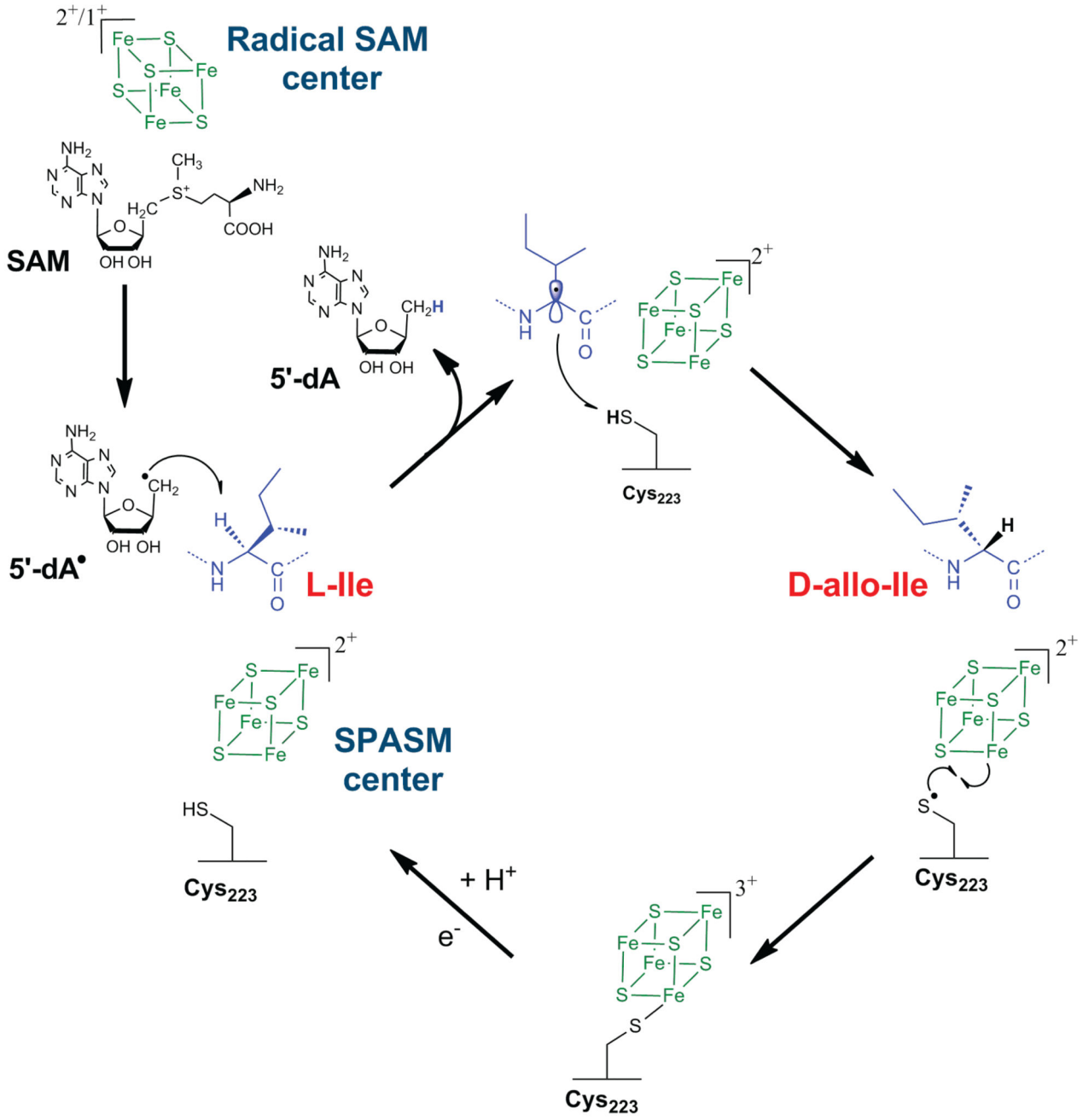

Figure 5. Proposed mechanism of the radical SAM peptide epimerase YydG.

YydG generates a 5′-dA• radical which abstracts an amino acid C_α H-atom. A carbon-centred radical is generated and quenched by the thiolate H-atom of Cys_{223} leading to the formation of a D-amino acid residue. The SPASM [4Fe-4S] center likely assists the radical quenching by reducing the thiyl radical. Further reduction of Cys_{223} would be required to allow another catalytic cycle.

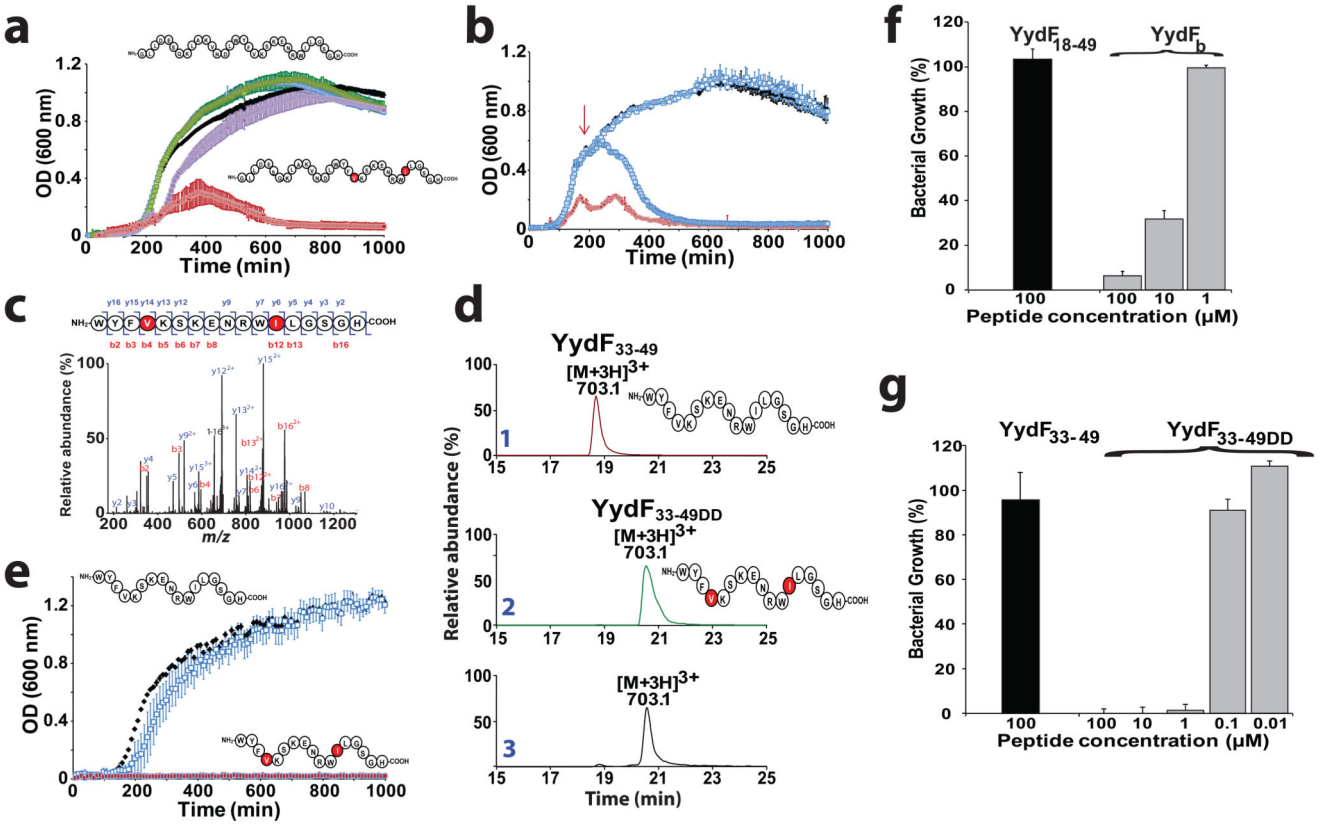

Figure 6. Activity of the epipeptides on *Bacillus subtilis*.

(**a**) **Growth of *B. subtilis* in liquid LB medium in the presence of $YydF_{18-49}$ or peptides containing one or two epimerized residues in position 36 and 44.** *B. subtilis* was grown in LB medium alone (black squares), in the presence of $YydF_{18-49}$ (white squares), $YydF_a$ (purple squares), $YydF_c$ (Green squares) or $YydF_b$ (red squares). Each measurement is the mean of three growth experiments with the SD indicated. (**b**) **Growth of *B. subtilis* in the presence of $YydF_{18-49}$ at initial time or mid-exponential phase.** *B. subtilis* was grown in LB medium alone (black squares), in the presence of $YydF_{18-49}$ (white squares), $YydF_b$ (red squares) or after addition of $YydF_b$ at mid-exponential phase (indicated by the red arrow) (light blue squares). Each measurement is the mean of three growth experiments with the SD indicated. **(c) LC-MS/MS analysis of the purified peptide from *B. subtilis*.** (*see* Supplementary methods *for peptide purification*). **(d) LC-MS analysis of $YydF_{33-49}$, $YydF_{33-49DD}$ synthetic peptides (traces 1&2) and the peptide isolated from *B. subtilis* (trace 3).** (*See* Supplementary Fig. S28 & S29 *for complete assignment*). **(e) Growth of *B. subtilis* in liquid LB medium in the presence of $YydF_{33-49DD}$.** *B. subtilis* was grown in LB medium alone (black squares), in the presence of $YydF_{33-49}$ (white squares) or $YydF_{33-49DD}$ (red squares). Each measurement is the mean of three growth experiments with the SD indicated. **Growth ratio of *B. subtilis* in the presence of (f) $YydF_{18-49}$ (100 μM) or $YydF_b$ and (g) $YydF_{33-49}$ or $YydF_{33-49DD}$.** Ratios were determined by comparison with growth in the absence of peptide.

Europe PMC Funders Author Manuscripts